

CSCNET: CLASS-SPECIFIED CASCADED NETWORK FOR COMPOSITIONAL ZERO-SHOT LEARNING

Yanyi Zhang¹, Qi Jia¹, Xin Fan¹, Yu Liu^{1*}, Ran He^{2*}

¹ International School of Information Science and Engineering, Dalian University of Technology, China
² MAIS&CRIPAC, Institute of Automation, Chinese Academy of Sciences, China

ABSTRACT

Attribute and object (A-O) disentanglement is a fundamental and critical problem for Compositional Zero-shot Learning (CZSL), whose aim is to recognize novel A-O compositions based on foregone knowledge. Existing methods based on disentangled representation learning lose sight of the contextual dependency between the A-O primitive pairs. Inspired by this, we propose a novel A-O disentangled framework for CZSL, namely Class-specified Cascaded Network (CSCNet). The key insight is to firstly classify one primitive and then specifies the predicted class as a priori for guiding another primitive recognition in a cascaded fashion. To this end, CSCNet constructs Attribute-to-Object and Object-to-Attribute cascaded branches, in addition to a composition branch modeling the two primitives as a whole. Notably, we devise a parametric classifier (ParamCls) to improve the matching between visual and semantic embeddings. By improving the A-O disentanglement, our framework achieves superior results than previous competitive methods.

Index Terms— Compositional Zero-shot Learning, Disentangled Representation, Cascaded Network

1. INTRODUCTION

The hallmark of human cognitive system is compositionality, which enables us to effortlessly reason about unknown categories by recomposing existing concepts. Inspired by this, Compositional Zero-shot Learning (CZSL) [1, 2, 3] is proposed to make the machines recognize novel attribute-object (A-O) compositions by acquiring knowledge from known ones, as shown in the top of Fig. 1.

The core in CZSL is how to isolate attribute and object information from a unified visual feature. Most methods [4, 5, 6, 7, 8, 9, 10], address this problem through disentangled representation learning, which builds two independent primitive recognition branches separately, see “Baseline” in Fig. 1. However, these methods overlook the contextual dependency between A-O during primitive modeling, leading to less generalizability on novel and unseen compositions. Recently,

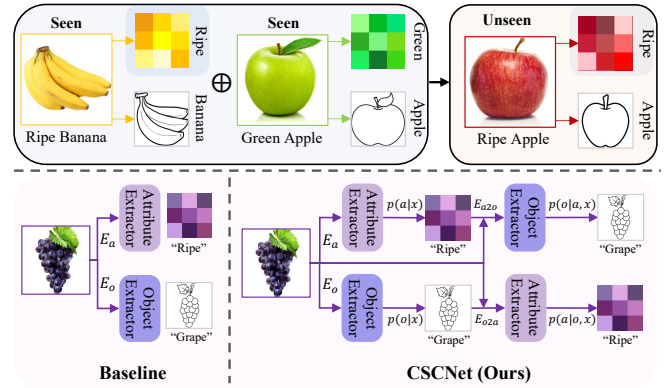


Fig. 1. Top: concept illustration of CZSL, where a novel composition “Ripe Apple” recomposes attribute and object primitives learned from known compositions “Ripe Banana” and “Green Apple”. Bottom: comparing the A-O disentanglement between the baseline method and CSCNet we propose. Note that, we omit the composition branch for brevity.

SeCoNet [11] proposed to utilize the decoupled feature maps of the first primitive to guide the second primitive decoupling network, facilitating the inducement between them. However, their inducement is overly restrictive, resulting in less accurate prediction of the second primitive. Another work similar to ours, called CANet [12], proposed to leverage object classification results to induce the semantic embeddings of attributes, whereas it neglects the contextuality of the object. For instance, the visual features of potato in mashed potato differ from those of peeled potato.

To conquer the limitations above, we propose a novel A-O disentangled framework termed Class-specified Cascaded Network (CSCNet), as sketched in Fig. 1. Different from previous methods, we exploit class-specified guidance to model both attribute-to-object and object-to-attribute dependency simultaneously. Concretely, the model constructs an attribute-to-object (A2O) cascaded branch, where it firstly classifies the attribute and then specifies the predicted class as a priori to guide the object recognition. A contrary pipeline takes place in a object-to-attribute (O2A) cascaded branch. Notably, we devise a parametric classifier (ParamCls) for matching visual-

*equal corresponding author.

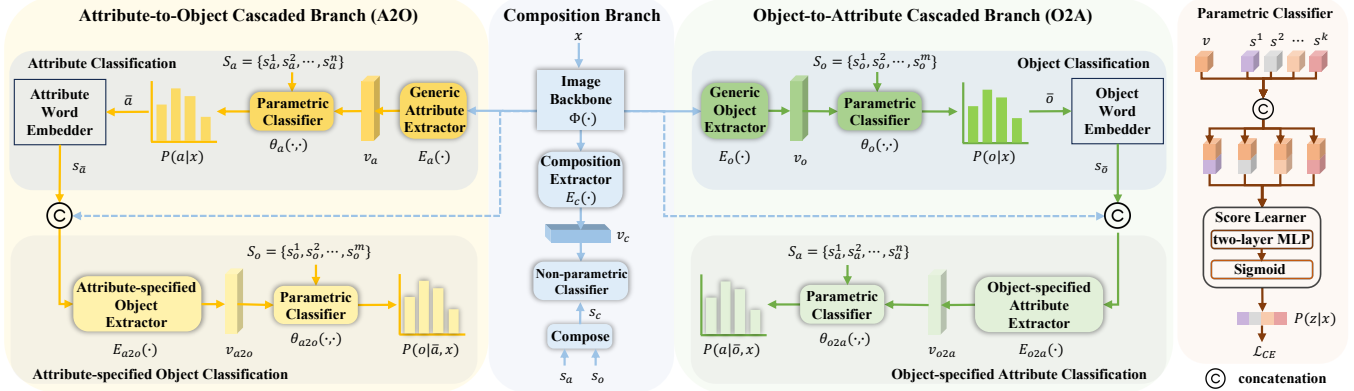


Fig. 2. Architecture of our Class-specified Cascaded Network (CSCNet) for CZSL.

semantic embeddings in A2O and O2A branches. Advantageously, our ParamCls develops a score learner to learn optimal matching scores, instead of using the traditional non-parametric manner based cosine score. In addition, a composition branch is also available for modeling the two primitives as a whole. In summary, our contributions are three-fold: 1) we develop a novel A-O disentanglement framework modeling contextual dependency with class-specified guidance; 2) we design a parametric classifier to learn optimal matching scores between visual and semantic embeddings; 3) extensive results on two datasets demonstrate CSCNet achieves superior performance compared to previous competitive methods.

2. METHODOLOGY

Overview. Fig. 2 depicts the architecture of CSCNet for CZSL. Given an image instance, we extract the image feature with a pre-trained backbone. The feature is then fed into the attribute-to-object cascaded branch (A2O), object-to-attribute cascaded branch (O2A), and composition branch. A2O firstly classifies the attribute and then specifies the predicted class as a priori to guide the object classification. Likewise, O2A classifies objects and then uses the results to guide attribute classification. The composition branch classifies A-O pairs as a whole, so as to capture intricate A-O entanglement. The three branches can be trained jointly.

2.1. Attribute-to-Object Cascaded Branch (A2O)

Attribute Classification. After obtaining the image feature $\Phi(x)$ extracted by an image backbone $\Phi(\cdot)$, we feed it into a generic attribute extractor $E_a(\cdot)$. As a result, a disentangled attribute visual feature v_a is achieved by $v_a = E_a(\Phi(x))$. On the other hand, we have the ground-truth attribute labels and capture their semantic embeddings from a language encoder like word2vec [13], denoted as $S_a = \{s_a^1, s_a^2, \dots, s_a^n\}$, where S_a represents the semantic features of all attributes and n is the number of attribute classes. For attribute classification, it is important to compute the matching scores between visual

and semantic embeddings. In general, existing methods employ a simple non-parametric manner based on cosine scores. On the contrary, we propose to devise a **parametric classifier (ParamCls)** which leverages a score learner to make the matching scores be learnable, together with other network parameters. As shown in the right of Fig. 2, we concatenate v_a with each s_a^i and then feed them into a score learner, which consists of a two-layer Multilayer Perceptron (MLP) followed by a Sigmoid function. Formally, the computation in ParamCls is given by

$$\theta_a(v_a, S_a) = \text{Sigmoid}(\text{MLP}(\text{Concat}(v_a, S_a))), \quad (1)$$

where $\theta_a(\cdot, \cdot)$ outputs the attribute classification probabilities with ParamCls. Based on the matching scores, we compute the cross-entropy loss \mathcal{L}_a for attribute classification:

$$\mathcal{L}_a = -y_a \log P(a | x) = -y_a \log \theta_a(v_a, S_a), \quad (2)$$

where one-hot vector y_a represents the attribute ground-truth of x . Note that, we omit the index i in $\{(x^i, y_a^i)\}_{i=1}^N$ for brevity. After estimating the predicted attribute label \bar{a} , we further capture its corresponding semantic embedding $s_{\bar{a}}$ via an attribute word embedder, for example $s_{\bar{a}} = \text{word2vec}(\bar{a})$. Importantly, $s_{\bar{a}}$ will guide the following object classification.

Attribute-specified Object Classification. To grasp the contextual dependency between attributes and objects, we specify the predicted attribute label as a priori to guide the object classification. Intuitively, when the attribute label is provided, it becomes easier to predict the remaining object label. To make it, we firstly concatenate the semantic embedding $s_{\bar{a}}$ with the image feature $\Phi(x)$. Then we pass the resulting feature to a new attribute-specified object extractor $E_{a2o}(\cdot)$ and derive object visual feature v_{a2o} :

$$v_{a2o} = E_{a2o}(\text{Concat}(\Phi(x), s_{\bar{a}})). \quad (3)$$

Likewise, we proceed to perform object classification by learning a new ParamCls $\theta_{a2o}(\cdot, \cdot)$ and calculate the cross-entropy loss \mathcal{L}_{a2o} :

$$\mathcal{L}_{a2o} = -y_o \log P(o | \bar{a}, x) = -y_o \log \theta_{a2o}(v_{a2o}, S_o), \quad (4)$$

where $P(o | \bar{a}, x)$ is the classification probabilities of an object given attribute prediction \bar{a} , one-hot vector y_o indicates the object ground-truth, and $S_o = \{s_o^1, s_o^2, \dots, s_o^m\}$ denotes the semantic embeddings of all objects. In a nutshell, the tasks of attribute and object classification are linked seamlessly through a cascaded fashion.

2.2. Object-to-Attribute Cascaded Branch (O2A)

Similar to A2O, we first perform object classification and then proceed to attribute classification. Specifically, we decouple the object visual features v_o by a generic object extractor $E_o(\cdot)$, i.e. $v_o = E_o(\Phi(x))$. The loss for this object classification task is formulated as:

$$\mathcal{L}_o = -y_o \log P(o | x) = -y_o \log \theta_o(v_o, S_o). \quad (5)$$

Subsequently, we convert the object classification result \bar{o} to semantic embedding $s_{\bar{o}}$ and specify it as a priori for the following attribute classification. We merge $s_{\bar{o}}$ with $\Phi(x)$ for deriving attribute embedding v_{o2a} from object-specified attribute extractor $E_{o2a}(\cdot)$. Finally, we match v_{o2a} with S_a by using ParamCls $\theta_{o2a}(\cdot, \cdot)$ and achieve the loss cost \mathcal{L}_{o2a} :

$$\mathcal{L}_{o2a} = -y_a \log P(a | \bar{o}, x) = -y_a \log \theta_{o2a}(v_{o2a}, S_a). \quad (6)$$

2.3. Composition Branch

Although we have performed precise classification of individual primitives, it is still necessary to learn the composition as a whole. This is because there is an intricate entanglement between A-O, and modeling this entanglement is crucial for preserving the contextuality. Hence, we encode the image feature $\Phi(x)$ to obtain a composition visual features $v_c = E_c(\Phi(x))$, where $E_c(\cdot)$ denotes a composition extractor. Then, we compose the primitive semantic embeddings (i.e. s_a and s_o) into a composition semantic embedding s_c by

$$s_c = \text{Compose}(s_a, s_o) = \text{MLP}(\text{Concat}(s_a, s_o)). \quad (7)$$

Subsequently, we utilize a non-parametric classifier (Non-PaCls) based on cosine score, for matching v_c and s_c . We need to note that ParamCls is not suitable for composition classification. The reason is that the test set contains some unseen compositions that cannot be learned by ParamCls in advance during training. Using ParamCls for composition classification may lead the model to being biased on seen compositions during inference. Differently, since all the objects and attributes have been seen at training phase for CZSL, ParamCls is undoubtedly suitable for attribute and object classification. Finally, the composition classification loss \mathcal{L}_c is

$$\mathcal{L}_c = -y_c \log P(c | x) = -\log \frac{\exp \langle v_c, s_c \rangle}{\sum_{s_{\hat{c}} \in S_c} \exp \langle v_c, s_{\hat{c}} \rangle}, \quad (8)$$

where $\langle \cdot, \cdot \rangle$ denotes cosine similarity and S_c includes the semantic embeddings of all compositions.

Table 1. Comparison with state-of-the-art results on MIT-States and C-GQA. The best results are shown in **bold**.

Dataset →	MIT-States				C-GQA				
	Method ↓	AUC	HM	Seen	Unseen	AUC	HM	Seen	Unseen
AttrAsOp [14]	1.6	9.9	14.3	17.4	0.7	5.9	17.0	5.6	
TMN [15]	2.9	13.0	20.2	20.1	1.1	7.5	23.1	6.5	
SymNet [16]	3.0	16.1	24.4	25.2	2.1	11.0	26.8	10.3	
SeCoNet [11]	4.0	17.4	26.0	24.8	1.3	7.7	21.8	7.8	
CompCos [17]	4.5	16.4	25.3	24.6	2.6	12.4	28.1	11.2	
CGE [18]	5.1	17.2	28.7	25.3	2.3	11.4	28.1	10.1	
IVR [6]	-	-	-	-	2.2	10.9	27.3	10.0	
SRA [19]	5.2	17.9	29.2	24.0	2.2	11.0	26.4	10.8	
SCEN [20]	5.3	18.4	29.9	25.2	2.9	12.4	28.9	12.1	
DeCa [8]	5.3	18.2	29.8	25.2	-	-	-	-	
CANet [12]	5.4	17.9	29.0	26.2	3.3	14.5	30.0	13.2	
CSCNet (Ours)	5.7	18.4	30.0	26.2	3.4	14.4	30.4	13.4	

2.4. Training and Inference

All the three branches in CSCNet can be trained jointly. The total loss is a combination of five loss terms as follows:

$$\mathcal{L}_{total} = \alpha(\mathcal{L}_a + \mathcal{L}_o + \mathcal{L}_{a2o} + \mathcal{L}_{o2a}) + \mathcal{L}_c, \quad (9)$$

where α weighs the loss cost in A2O and O2A. During inference, we integrate the probabilities from the three branches. The final score is calculated by the formula below:

$$\begin{aligned} \text{Score} = & \beta(P(a | x)P(o | \bar{a}, x) + P(o | x)P(a | \bar{o}, x)) \\ & + (1 - \beta)P(c | x), \end{aligned} \quad (10)$$

where β is a trade-off hyper-parameter.

3. EXPERIMENTS

3.1. Dataset and Details

We conduct experiments on two datasets, MIT-States [21] and C-GQA [18]. CZSL is commonly evaluated by four metrics: AUC, HM, Seen, and Unseen. Seen and Unseen metrics quantify the model’s maximum predictive capability over seen and unseen compositions, while AUC and HM metrics assess the holistic performance [22]. Following the literature, we employ ResNet-18 [23] pre-trained on ImageNet [24] as the image backbone. Each of the feature extractors is a two-layer MLP, without sharing the parameters. The semantic features are parameterized by word2vec+fasttext [13, 25] for MIT-States and by word2vec for C-GQA. CSCNet is trained using the Adam optimizer [26] with a learning rate of 5.0×10^{-5} for both datasets with 300 epochs on MIT-States and 200 epochs on C-GQA. The batch size is 256 on MIT-States and 128 on C-GQA. α is set to 4 on both datasets. β is 0.1 on MIT-States and 0.2 on C-GQA. Experiments were conducted on a single NVIDIA RTX 3090 GPU card.

Table 2. Ablation study on A2O and O2A in C-GQA.

Method	AUC	HM	Seen	Unseen
Composition Branch	2.7	12.8	29.4	11.4
+ Only A2O	3.1	13.4	30.3	12.5
+ Only O2A	3.0	13.4	30.5	12.5
+ A2O and O2A	3.4	14.4	30.4	13.4

Table 3. Ablation study on ParamCls in C-GQA.

Model	A2O & O2A	Composition	AUC	HM	Seen	Unseen
M_1	NonPaCls	NonPaCls	3.0	13.3	29.9	12.3
M_2	ParamCls	ParamCls	2.8	12.9	29.3	11.7
M_3	NonPaCls	ParamCls	2.7	12.8	28.9	11.9
M_4	ParamCls	NonPaCls	3.4	14.4	30.4	13.4

3.2. Comparison with State-of-the-arts

We provide a comprehensive comparison with competitive methods including SecoNet [11] and CANet [12]. Table 1 reports the compared results on two datasets. Overall, CSCNet achieves the best results across all metrics for both datasets, except 0.1 lower than CANet on HM for C-GQA. Notably, our AUC results, that is 5.7 in MIT-States and 3.4 in C-GQA, represent 5.6% and 3.0% gains over previous state-of-the-art methods. Besides, CSCNet exhibits significant improvements on Seen and Unseen metrics, surpassing existing methods with a consistent margin.

3.3. Ablation Study and Analysis

Effectiveness of A2O and O2A. First of all, we implement a basic model with the composition branch only. Then we add more branches on top of this basic model to study the effectiveness of A2O and O2A. As shown in Tab. 2, equipping the model with either A2O or O2A improves all the metrics, compared to using the composition branch only. Moreover, when both A2O and O2A are deployed, the model outperforms the counterparts with only A2O or O2A and achieves the best performance. It verifies that the exploration of A-O dependency benefits disentangled representation learning.

Effectiveness of parametric classifier. As discussed in Section 2.3, ParamCls is suitable for both A2O and O2A branches, but not for the composition branch. To prove it, we conduct this ablation experiment as shown in Tab. 3. When comparing M_4 with M_1 , we can observe that using ParamCls for A2O and O2A, instead of non-parametric classifier (*i.e.* NonPaCls), brings considerable boosts for all the metrics. However, when ParamCls is applied to the composition branch, *i.e.* M_2 and M_3 , the performance is even inferior to that of M_1 . These results further verify our explanation about why ParamCls is not suitable for the composition branch.

Impact of β on inference. Inspired by [27, 28], this experiment studies the impact of tuning the hyper-parameter β in Eq. 10 during inference. As shown in Fig. 3, the AUC accu-

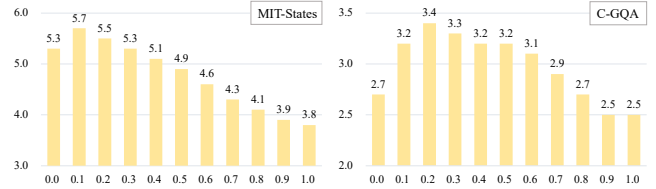


Fig. 3. Impact of β on AUC accuracy for two datasets.



Fig. 4. Qualitative Results on MIT-States (Top) and C-GQA (Bottom). We present Top-3 prediction candidates using CSCNet, where green indicates correct predictions and yellow indicates incorrect predictions.

racy exhibits a trend of initially increasing and then decreasing on both datasets. Finally, CSCNet achieves the best performance when β is 0.1 for MIT-States and 0.2 for C-GQA, respectively.

3.4. Qualitative Analysis

Fig. 4 shows several Top-3 prediction candidates of CSCNet on MIT-States (Top) and C-GQA (Bottom). We can see that the first candidate precisely match the ground-truth. In addition, the second and third candidates still contain the correct primitives (attributes or objects) or their synonyms. It is evident that the results can still accurately describe the image.

4. CONCLUSION

In this work, in order to model the contextual dependency, we have proposed a novel A-O disentanglement framework named Class-specified Cascaded Network (CSCNet). Specifying the result of the attribute classification as a priori, we further guide the object classification in a cascaded fashion. Simultaneously, we classify attributes under the guidance of object classification. In addition, we employ a parametric classifier to learn optimal matching scores. Experiments and ablation studies on two datasets demonstrate the superiority of our method. In future work, it is promising to apply CSCNet to a open-world CZSL setting.

5. REFERENCES

- [1] Ishan Misra, Abhinav Gupta, and Martial Hebert, “From red wine to red tomato: Composition with context,” in *Proc. of the CVPR*, 2017, pp. 1160–1169.
- [2] Kun Wei, Muli Yang, Hao Wang, Cheng Deng, and Xianglong Liu, “Adversarial fine-grained composition learning for unseen attribute-object recognition,” in *Proc. of the ICCV*, 2019, pp. 3740–3748.
- [3] Yuval Atzmon, Felix Kreuk, Uri Shalit, and Gal Chechik, “A causal view of compositional zero-shot recognition,” in *the NeurIPS*, 2020.
- [4] Yanhua Yang, Rui Pan, Xiangyu Li, Xu Yang, and Cheng Deng, “Dual-stream contrastive learning for compositional zero-shot recognition,” *IEEE Transactions on Multimedia*, 2023.
- [5] Nan Pu, Wei Chen, Yu Liu, Erwin M. Bakker, and Michael S. Lew, “Dual gaussian-based variational subspace disentanglement for visible-infrared person re-identification,” in *ACM MM*, 2020, pp. 2149–2158.
- [6] Tian Zhang, Kongming Liang, Ruoyi Du, Xian Sun, Zhanyu Ma, and Jun Guo, “Learning invariant visual representations for compositional zero-shot learning,” in *Proc. of the ECCV*, 2022, pp. 339–355.
- [7] Nirat Saini, Khoi Pham, and Abhinav Shrivastava, “Disentangling visual embeddings for attributes and objects,” in *Proc. of the CVPR*, 2022, pp. 13658–13667.
- [8] Muli Yang, Chenghao Xu, Aming Wu, and Cheng Deng, “A decomposable causal view of compositional zero-shot learning,” *IEEE Transactions on Multimedia*, pp. 1–11, 2022.
- [9] Ziwei Xu, Guangzhi Wang, Yongkang Wong, and Mohan S. Kankanhalli, “Relation-aware compositional zero-shot learning for attribute-object pair recognition,” *IEEE Transactions on Multimedia*, vol. 24, pp. 3652–3664, 2022.
- [10] Nan Pu, Wei Chen, Yu Liu, Erwin M. Bakker, and Michael S. Lew, “Lifelong person re-identification via adaptive knowledge accumulation,” in *Proc. of the CVPR*, 2021, pp. 7901–7910.
- [11] Aditya Panda, Bikash Santra, and Dipti Prasad Mukherjee, “Isolating features of object and its state for compositional zero-shot learning,” *IEEE Transactions on Emerging Topics in Computational Intelligence*, pp. 1–13, 2023.
- [12] Qingsheng Wang, Lingqiao Liu, Chenchen Jing, Hao Chen, Guoqiang Liang, Peng Wang, and Chunhua Shen, “Learning conditional attributes for compositional zero-shot learning,” in *Proc. of the CVPR*, 2023, pp. 11197–11206.
- [13] Tomas Mikolov, Kai Chen, Greg Corrado, and Jeffrey Dean, “Efficient estimation of word representations in vector space,” in *Proc. of the ICLR*, 2013.
- [14] Tushar Nagarajan and Kristen Grauman, “Attributes as operators: Factorizing unseen attribute-object compositions,” in *Proc. of the ECCV*, 2018, pp. 172–190.
- [15] Senthil Purushwalkam, Maximilian Nickel, Abhinav Gupta, and Marc’Aurelio Ranzato, “Task-driven modular networks for zero-shot compositional learning,” in *Proc. of the ICCV*, 2019, pp. 3592–3601.
- [16] Yong-Lu Li, Yue Xu, Xiaohan Mao, and Cewu Lu, “Symmetry and group in attribute-object compositions,” in *Proc. of the CVPR*, 2020, pp. 11313–11322.
- [17] Massimiliano Mancini, Muhammad Ferjad Naeem, Yongqin Xian, and Zeynep Akata, “Open world compositional zero-shot learning,” in *Proc. of the CVPR*, 2021, pp. 5222–5230.
- [18] Muhammad Ferjad Naeem, Yongqin Xian, Federico Tombari, and Zeynep Akata, “Learning graph embeddings for compositional zero-shot learning,” in *Proc. of the CVPR*, 2021, pp. 953–962.
- [19] T. Guo, J. Liang, and G. Xie, “Swap-reconstruction autoencoder for compositional zero-shot learning,” in *Proc. of the ICME*, 2023, pp. 438–443.
- [20] Xiangyu Li, Xu Yang, Kun Wei, Cheng Deng, and Muli Yang, “Siamese contrastive embedding network for compositional zero-shot learning,” in *Proc. of the CVPR*, 2022, pp. 9326–9335.
- [21] Phillip Isola, Joseph J. Lim, and Edward H. Adelson, “Discovering states and transformations in image collections,” in *Proc. of the CVPR*, 2015, pp. 1383–1391.
- [22] Shaozhe Hao, Kai Han, and Kwan-Yee K. Wong, “Learning attention as disentangler for compositional zero-shot learning,” in *Proc. of the CVPR*, 2023, pp. 15315–15324.
- [23] Kaiming He, Xiangyu Zhang, Shaoqing Ren, and Jian Sun, “Deep residual learning for image recognition,” in *Proc. of the CVPR*, 2016, pp. 770–778.
- [24] Jia Deng, Wei Dong, Richard Socher, Li-Jia Li, Kai Li, and Li Fei-Fei, “Imagenet: A large-scale hierarchical image database,” in *Proc. of the CVPR*, 2009, pp. 248–255.

- [25] Piotr Bojanowski, Edouard Grave, Armand Joulin, and Tomáš Mikolov, “Enriching word vectors with subword information,” *Trans. Assoc. Comput. Linguistics*, vol. 5, pp. 135–146, 2017.
- [26] Diederik P. Kingma and Jimmy Ba, “Adam: A method for stochastic optimization,” in *Proc. of the ICLR*, 2015.
- [27] Nan Pu, Yu Liu, Wei Chen, Erwin M. Bakker, and Michael S. Lew, “Meta reconciliation normalization for lifelong person re-identification,” in *ACM MM*, 2022, pp. 541–549.
- [28] Nan Pu, Zhun Zhong, Nicu Sebe, and Michael S. Lew, “A memorizing and generalizing framework for lifelong person re-identification,” *IEEE Transactions on Pattern Analysis and Machine Intelligence*, vol. 45, no. 11, pp. 13567–13585, 2023.